Behavioral/Systems/Cognitive

Hyperdopaminergia and NMDA Receptor Hypofunction Disrupt Neural Phase Signaling

Kafui Dzirasa,[1] Amy J. Ramsey,[2] Daniel Yasumasa Takahashi,[6,7] Jennifer Stapleton,[1] Juan M. Potes,[1] Jamila K. Williams,[1] Raul R. Gainetdinov,[2] Koichi Sameshima,[6,7] Marc G. Caron,[2] and Miguel A. L. Nicolelis[1,3,4,5,6]

Departments of [1]Neurobiology, [2]Cell Biology, [3]Psychology and Neuroscience, and [4]Biomedical Engineering and [5]Center for Neuroengineering, Duke University Medical Center, Durham, North Carolina 27710, [6]Edmond and Lily Safra International Institute of Neuroscience of Natal, 59066-060 Natal, Brazil, and [7]Bioinformatics Graduate Program and Department of Radiology, School of Medicine, University of São Paulo, 01246-903 São Paulo SP, Brazil

Neural phase signaling has gained attention as a putative coding mechanism through which the brain binds the activity of neurons across distributed brain areas to generate thoughts, percepts, and behaviors. Neural phase signaling has been shown to play a role in various cognitive processes, and it has been suggested that altered phase signaling may play a role in mediating the cognitive deficits observed across neuropsychiatric illness. Here, we investigated neural phase signaling in two mouse models of cognitive dysfunction: mice with genetically induced hyperdopaminergia [dopamine transporter knock-out (DAT-KO) mice] and mice with genetically induced NMDA receptor hypofunction [NMDA receptor subunit-1 knockdown (NR1-KD) mice]. Cognitive function in these mice was assessed using a radial-arm maze task, and local field potentials were recorded from dorsal hippocampus and prefrontal cortex as DAT-KO mice, NR1-KD mice, and their littermate controls engaged in behavioral exploration. Our results demonstrate that both DAT-KO and NR1-KD mice display deficits in spatial cognitive performance. Moreover, we show that persistent hyperdopaminergia alters interstructural phase signaling, whereas NMDA receptor hypofunction alters interstructural and intrastructural phase signaling. These results demonstrate that dopamine and NMDA receptor dependent glutamate signaling play a critical role in coordinating neural phase signaling, and encourage further studies to investigate the role that deficits in phase signaling play in mediating cognitive dysfunction.

Introduction

Neural phase signaling has gained attention as a putative coding mechanism through which the brain binds the activity of neurons across brain structures to generate percepts and behaviors (Lisman and Buzsáki, 2008). For example, the synchronization of hippocampal and prefrontal cortical theta oscillations (4–10 Hz) is enhanced during spatial navigation in rodents (Jones and Wilson, 2005). The synchronization of hippocampal and amygdalar oscillations may play a role in fear conditioning (Seidenbecher et al., 2003), and the phase synchronization of rhinal and hippocampal gamma (33–55 Hz) oscillations has been suggested to coordinate memory formation (Fell et al., 2001). Moreover, some authors have reported that the long-range phase synchronization of cortical gamma oscillations underlies processes such as perception (Rodriguez et al., 1999). Together, these studies suggest that the long-range phase synchronization of theta and gamma oscillatory activity may play a role in coordinating interstructural neural activity.

Studies in rodents have also shown that neural activity within brain structures is coordinated by the phasic interaction of theta and gamma oscillations in which the amplitude of gamma oscillations is modulated by the phase of theta oscillations [cross frequency phase coupling (CFPC)] (Bragin et al., 1995; Chrobak and Buzsáki, 1998). More recently, it has been shown that phasic interactions between theta and gamma oscillations also coordinate neural activity across brain structures (Sirota et al., 2008). Importantly, studies have shown that phasic interactions between theta and gamma oscillations occur across the human neocortex as well (Palva et al., 2005; Canolty et al., 2006). These studies also demonstrate that theta-gamma coupling strength increases with cognitive load, suggesting that CFPC plays a role in coordinating neural oscillatory activity during high-end cognitive processes. Multiple studies in rodents demonstrate that phase signaling also coordinates brain activity at the neuronal level (phase locking) (Jones and Wilson, 2005; Siapas et al., 2005). Thus together, long-range phase synchronization, CFPC, and phase locking could define a putative code in which phase signaling binds the activity of neurons across distributed brain structures to generate thoughts and behaviors. Several studies in rats have been aimed at investigating local field potential and single unit phase signaling across the hippocampus (HP)–prefrontal cortex (PF) pathway (Jones and Wilson, 2005; Siapas et al., 2005). These studies have demonstrated that both hippocampal and PF

Received April 13, 2009; revised May 18, 2009; accepted May 20, 2009.

This work was supported by funding from the Wakeman Foundation, Ruth K. Broad Foundation, and United Negro College Fund/Merck to K.D.; by Award Numbers R01-NS19576 and MH73853 from the National Alliance for Research on Schizophrenia and Depression and National Institutes of Health (NIH) to M.G.C.; and by Award Numbers P50MH060451 and R33NSO49534 from NIH to M.A.L.N. A.J.R. is the recipient of NIH KO1 Award DA-17703. The content is solely the responsibility of the authors and does not necessarily represent the official views of the National Institute on Deafness and Other Communication Disorders or the NIH. A special thanks to Freeman Hrabowski, Robert and Jane Meyerhoff, and the Meyerhoff Scholarship Program. We thank our colleagues Shih-Chieh Lin and Ranier Gutierrez for comments on this manuscript; G. Lehew for technical assistance; L. Oliveira, T. Jones, and G. Wood for miscellaneous support; and S. Halkiotis for proofreading of this manuscript.

Correspondence should be addressed to Kafui Dzirasa, Department of Neurobiology, Duke University Medical Center, Bryan Research Building, Durham, NC 27710. E-mail: dzirasa@neuro.duke.edu.

DOI:10.1523/JNEUROSCI.1773-09.2009

 0270-6474/09/298215-10$15.00/0

neurons phase lock to hippocampal theta oscillations during exploration, and that HP and PF theta oscillations phase synchronize during accurate spatial task performance, suggesting that phase signaling plays an important role in coordinating HP–PF network function.

Here, we investigated neural phase signaling in two mouse models of cognitive dysfunction: mice with genetically induced hyperdopaminergia and mice with genetically induced NMDA receptor hypofunction. To assess spatial cognitive processing in the two mouse models, mutant mice and their littermate controls were subjected to a radial arm maze special learning task. Additionally, mice from each group were surgically implanted with recording electrodes in HP and prelimbic cortex (PrL) (an anatomical subdivision of medial prefrontal cortex in rats) and HP–PF phase signaling was quantified while mice were in their home cage and while they explored a novel environment.

Materials and Methods

Dopamine transporter knock-out mice and NMDA receptor subunit-1 knockdown mice. Wild-type (WT) and dopamine transporter (DAT) knock-out (KO) littermates were generated from heterozygotes that had been backcrossed over 10 generations onto the C57BL/6J background. DAT-KO mice lack the gene encoding the plasma membrane transporter that regulates spatial and temporal extracellular dopamine (DA) signaling (Giros et al., 1996). Because of loss of the DAT, these mutants exhibit a persistent fivefold increase in extracellular striatal DA levels (Giros et al., 1996; Gainetdinov and Caron, 2003) and show locomotor hyperactivity, deficits in cognitive functions, deficits in sensorimotor gating, and altered hippocampal activity during awake behavioral periods (Giros et al., 1996; Gainetdinov et al., 1999; Dzirasa et al., 2006).

Functional NMDA receptors are composed of an essential NMDA receptor subunit, NR1, and one of four NR2 NMDA receptor subunits combined in an undetermined ratio to make a heteromeric receptor complex (Kutsuwada et al., 1992; Monyer et al., 1992). Although the global deletion of the NR1 subunit leads to perinatal lethality (Forrest et al., 1994; Li et al., 1994), mice genetically engineered to express only 10% of normal NR1 levels via hypomorphic mutation of *Grin1* survive until adulthood (Mohn et al., 1999). Mice were derived by first generating C57BL6 and 129SvJ congenic lines (backcrossed >12 generations). C57BL6 and 129SvJ mice that were heterozygous for the altered *Grin1* allele were then crossed to generate the F1 mice used for this study. Importantly, NR1-knockdown (NR1-KD) mice exhibit a 90% reduction in functional NMDA receptors compared with WT mice, and also display locomotor hyperactivity, deficits in sensorimotor gating, and aberrant social interactions (Mohn et al., 1999; Duncan et al., 2006).

Animal care and use. Mice were housed 3–5 per cage and maintained in a humidity- and temperature-controlled room with a 12 h light/dark cycle. Food and water was available *ad libitum*. All studies were conducted with approved protocols from the Duke University Institutional Animal Care and Use Committee and were in accordance with the National Institutes of Health Guidelines for the Care and Use of Laboratory Animals.

Assessing spatial cognitive function using a radial arm maze learning task. Radial arm maze spatial learning experiments were conducted in 29 mice: 8 NR1-KD mice/7 WT littermate controls and 7 DAT-KO mice/7 WT litter mate controls. Mice were food deprived for ~5 h each day before task performance. After 1–2 shaping sessions, mice were subjected to five 4 d block trials (20 consecutive days) of the eight-arm radial maze task. Each trial consisted of confining the animal to the center of the maze for 1 min. After the confinement period, mice were allowed to explore the maze until 300 s elapsed or they entered all eight arms. Each arm was baited with a small piece of sweet breakfast cereal. Cognitive performance was then assessed by the mean number of entries to repeat, and the number of perseverative errors (the number of times an animal re-entered an arm that it had just left) observed in each animal during a trial block.

Electrophysiological recordings in mutant and WT mice. Five DAT-KO mice and seven WT littermate controls were separated into individual cages, and surgically implanted with microwire recording electrodes. Electrophysiological experiments were initiated after a 2 week recovery. Four WT and four DAT-KO mice were first subjected to electrophysiological recordings during periods of quiet waking in their home cage. Periods of quiet waking (behaviorally inactive) were identified using video recordings and local field potentials (LFP) power spectral analysis (Dzirasa et al., 2006). Subsequently, five WT mice and five DAT-KO mice were subjected to electrophysiological recordings as they explored a novel environment. A radial arm maze was chosen as the "novel environment" used for electrophysiological recordings in DAT-KO mice because radial arm maze exposure does not induce hyperactivity in these mice (Gainetdinov et al., 1999).

Five NR1-KD mice and four WT littermate controls were also separated into individual cages, and surgically implanted with recording electrodes. Experiments were initiated after a 2 week recovery. All of the WT mice were recorded during quiet waking in their home cage, and as they explored a novel environment. All of the NR1-KD mice were recorded as they explored a novel environment, and three of the mice were also recorded during quiet waking in their home cage. The novel environment used in NR1-KD and their littermate controls consisted of an open field (two NR1-KD and two WT controls) or radial arm maze (three NR1-KD and two WT controls). Both open field and radial arm maze exposure induced hyperactivity in NR1-KD mice. NR1-KD mice displayed mild seizure-like neural activity across HP and PrL (see supplemental Fig. S4, available at www.jneurosci.org as supplemental material). A subset of these mice also showed full generalized tonic-clonic seizures (A. J. Ramsey, unpublished observations). This latter group of mice was excluded from the study.

Surgery. DAT-KO mice and WT littermate controls were anesthetized with ketamine (100 mg/kg) and xylazine (10 mg/kg), placed in a stereotaxic device, and metal ground screws were secured to the cranium. Two 16-tungsten microwire array electrodes (30 μm diameter single wires) were implanted bilaterally through a small cranial window into the dorsal HP [stereotaxic coordinates: −2.3 mm anteroposterior (AP), +/−1.6 mm mediolateral (ML), and 1.5 mm dorsoventral (DV) from bregma], and anchored to ground screws located above the above the cortex using dental acrylic. Two 16-tungsten microwire array electrodes (30 μm diameter single wires) were also implanted bilaterally through a small cranial window into prelimbic cortex (stereotaxic coordinates: 1.7 mm AP, +/−0.4 mm ML, and 1.9 mm DV from bregma, and 2.7 mm AP, +/−0.4 mm ML, and 0.8 mm DV from bregma), and anchored to the secured ground screws using dental acrylic. The surgical procedure was identical for the NR1-KD mice and their littermate controls with the exception that the anesthetic dose was reduced by 50% for NR1-KD mice, and only one 16-tungsten microwire array electrode was implanted into the dorsal HP and one 12-tungsten microwire array electrode was implanted into PrL.

Neuronal and LFP data acquisition. Neural activity was recorded using the Multi-Neuron Acquisition Processor system (Plexon). LFPs were preamplified (500×), filtered (0.5–400 Hz), and digitized at 500 Hz using a Digital Acquisition card (National Instruments) and a Multi-Neuron Acquisition Processor (Plexon). All electrophysiological recordings were referenced to two ground screws, and recording segments demonstrating LFP saturation resulting from movement artifacts were excluded from analysis. It is important to note that LFP recordings were associated with significant phase offsets that varied across frequencies (Nelson et al., 2008). These phase offsets were corrected using the LFPAlign function (Plexon).

Behaviors were recorded with a video cassette recorder. Video images were loaded onto a cassette recorder and synchronized with the neural recordings using a millisecond-precision timer.

Determination of cross-structural phase synchrony. Ten to 16 LFPs were recorded per session (up to eight from HP and up to eight from prelimbic cortex). LFPs were filtered using butterworth bandpass filters designed to isolate either theta (4–10 Hz) or gamma (33–55 Hz) oscillations. The instantaneous phase of the filtered LFP was then determined using the Hilbert transform (Siapas et al., 2005), yielding two phase time series for each frequency, $\phi_{HP}(t)$ and $\phi_{PrL}(t)$ (500 values per second). The Rayleigh test of circular uniformity (Siapas et al., 2005; Jacobs et al., 2007) was then used to quantify phase synchrony as a function of the difference between the two phase time

series [$\phi_{HP}(t) - \phi_{PrL}(t)$]. We also used the Rayleigh test to quantify phase synchrony when time offsets ranging from −3 to 3 s in 20 ms increments were introduced between the phase time series. This yielded a total of 301 *Z*-statistic (stat) values, where *Z*-stat = $-\ln(P)$. The *Z*-stat value corresponding to phase synchrony was then given by the difference between the *Z*-stat at zero offset and the maximum *Z*-stat observed in the [−3 to −1 s] and [1 to 3 s] offset windows. This process was repeated for each of the up to 64 HP × PrL LFP combinations (8 HP channels × 8 PrL channels) recorded per mouse. The significance threshold for phase synchrony was then conservatively set at $\alpha = 0.001/(301*64*5\text{mice})$, corresponding to *Z*-stat = 18.38. All comparison combinations were used to make statistical comparisons of theta and gamma band phase synchrony across genotypes. This conservative approach was taken given the large coefficient of variation (mean C.V. = 102%) across the *Z*-stat values observed across gamma frequency HP × PrL combinations within mice. The interstructural phase synchrony data presented in Figure 1 was collected from the WT littermate controls of DAT-KO mice.

Determination of LFP theta-gamma cross-frequency phase coupling and power. LFPs were filtered using butterworth bandpass filters designed to isolate either theta (4–10 Hz) or gamma (33–55 Hz) oscillations. The instantaneous amplitude and phase of the filtered LFPs were then determined using the Hilbert transform, and the modulation index was calculated using the MATLAB code provided by Canolty et al. (2006) Briefly, a continuous variable $z(t)$ is defined as a function of the instantaneous theta phase and instantaneous gamma amplitude such that $z(t) = A_G(t)*e^{i\phi_{TH}(t)}$, where A_G is the instantaneous gamma oscillatory amplitude, and $e^{i\phi_{TH}}$ is a function of the instantaneous theta oscillatory phase. A time lag is then introduced between the instantaneous amplitude and theta phase values such that z_{surr} is parameterized by both time and the offset between the two variables, $z_{surr} = A_{HG}(t+\tau)*e^{i\phi_{TH}(t)}$. The moldus of the first moment of $z(t)$, compared with the distribution of surrogate lengths, provides a measure of coupling strength. The normalized *z*-scored length, or modulation index, is then defined as $M_{NORM} = (M_{RAW} - \mu)/\sigma$, where M_{RAW} is the modulus of the first moment of $z(t)$, μ is the mean of the surrogate lengths, and σ is their SD. Importantly, M_{NORM} is a *Z*-score and can be used to determine the probability that a result would be caused by chance. The interstructural and intrastructural cross-frequency phase coupling data presented in Figure 2 was collected from the WT littermate controls of NR1-KD mice.

Theta and gamma oscillatory power was determined for each LFP by taking the mean of the amplitude envelope calculated for each of the theta and gamma filtered LFP traces.

Determination of coherence and partial directed coherence. The HP-PrL LFP combinations which demonstrated the strongest phase synchrony were used to estimate the coherence (Bendat and Piersol, 1986) and partial directed coherence (Sameshima and Baccalá, 1999; Baccalá and Sameshima, 2001) for each animal. Squared coherence is a frequency-wise measure of the total coupling strength between two waves. Squared coherence was calculated using previously described methods based on vector autoregressive (VAR) modeling (Bendat and Piersol, 1986; Baccalá et al., 2006). Briefly, the bivariate VAR model of order p is described by the following equation:

$$\begin{bmatrix} X_t^1 \\ X_t^2 \end{bmatrix} = \sum_{s=1}^{p} \begin{bmatrix} a_s^{11} & a_s^{12} \\ a_s^{21} & a_s^{22} \end{bmatrix} \begin{bmatrix} X_{t-s}^1 \\ X_{t-s}^2 \end{bmatrix} + \begin{bmatrix} \epsilon_t^1 \\ \epsilon_t^2 \end{bmatrix},$$

where X_t^m, $m = 1,2$ represents the *m*th time series at time *t* and σ_t^m, $m = 1,2$ is the *m*th innovation with covariance matrix

$$\sum = \begin{bmatrix} \sigma_{11} & \sigma_{12} \\ \sigma_{21} & \sigma_{22} \end{bmatrix}.$$

Important quantities are the bivariate autoregressive filter given by the following:

$$\begin{bmatrix} a^{11}(\lambda) & a^{12}(\lambda) \\ a^{21}(\lambda) & a^{22}(\lambda) \end{bmatrix} = \begin{bmatrix} 1 & 0 \\ 0 & 1 \end{bmatrix} - \sum_{s=1}^{p} \begin{bmatrix} a_s^{11} & a_s^{12} \\ a_s^{21} & a_s^{22} \end{bmatrix} e^{-2i\pi\lambda s},$$

and the bivariate spectral density matrix given by the following:

$$\begin{bmatrix} S^{11}(\lambda) & S^{12}(\lambda) \\ S^{21}(\lambda) & S^{22}(\lambda) \end{bmatrix} = \begin{bmatrix} a^{11}(\lambda) & a^{12}(\lambda) \\ a^{21}(\lambda) & a^{22}(\lambda) \end{bmatrix}^{-H} \sum \begin{bmatrix} a^{11}(\lambda) & a^{12}(\lambda) \\ a^{21}(\lambda) & a^{22}(\kappa) \end{bmatrix}^{-1},$$

where the superscript *H* stands for conjugate transpose operation, for any frequency $\lambda \in [-\eth, \eth)$.

The squared coherence at frequency λ between time series 1 and 2 is then given by the following:

$$|Coh(\lambda)|^2 = \frac{|S^{12}(\lambda)|^2}{S^{11}(\lambda)S^{22}(\lambda)}.$$

The modulus square of partial directed coherence (PDC) from signal 2 to 1, which will be discussed below can be written as follows:

$$|PDC_{2\to1}(\lambda)|^2 = \frac{|a^{12}(\lambda)|^2 \frac{1}{\sigma^{11}}}{|a^{12}(\lambda)|^2 \frac{1}{\sigma^{11}} + |a^{22}(\lambda)|^2 \frac{1}{\sigma^{22}}}.$$

The PDC from signal 1 to 2 can be written analogously.

For the analysis, a VAR model was fitted sequentially to each nonoverlapping 0.5 s time segments to assure a stationary and adequate fit. The coherence for each animal was then calculated as the average of the squared coherences calculated from each VAR model for each respective LFP recording. The averages for the WT and DAT-KO group coherences were calculated as the averages of the mean coherences for the mice in respective groups, and the total theta coherence was defined as the average of the squared coherence values in the 4–10 Hz range. Similarly, the total gamma coherence was defined as the average of squared coherence values in the 33–55 Hz range. The statistical distribution for the null hypothesis of zero total theta and gamma coherences were calculated by the parametric bootstrap method previously described (Baccalá et al., 2006).

PDC is an established method for the identification of directional interaction between brain areas (Sameshima and Baccalá, 1999; Baccalá and Sameshima, 2001; Baccalá et al., 2006; Takahashi et al., 2007). Briefly, consider two wave signals, $u1$ and u_2. PDC from u_1 to u_2 measures the proportion of the power spectra of u_2 resulting from an effect from u_1. Similarly, the PDC from u_2 to u_1 measures the proportion of the power spectra of u_1 resulting from an effect from u_2. The key property that allows for calculation of PDC is asymmetry between u_1 and u_2, such that the PDC from u_1 to u_2 is generally not equal to PDC from u_2 to u_1. Nullity of PDC from u_1 to u_2 indicates the absence of an influence of u_1 on u_2, and thus no directional interaction. Conversely, a PDC value of one determined from u_1 to u_2 indicates that u_2 is linearly predictable from u_1. A useful form of PDC called generalized PDC was used for all PDC computations presented in the text (Baccalá et al., 2006). PDC was computed with the same VAR models used to calculate coherence. The same procedures used to estimate the total theta and gamma coherences were used to estimate the WT and DAT-KO group total theta and gamma PDC. Parametric bootstrap analysis was used to calculate the threshold values under the null hypothesis of zero total theta and gamma PDC (Baccalá et al., 2006).

Statistics. Statistical significance was determined for interstructural phase synchrony and interstructural CFPC comparisons across genotype using a Bonferroni corrected two-tailed *t* test. The significance threshold was conservatively estimated at $\alpha = 0.001/(64\text{-combinations}*10\text{-mice})$ or $p < 0.000001$. Statistical significance was determined for intrastructure cross- frequency phase coupling using ANOVA followed by Student's *t* test. In this case, we conservatively corrected for six comparisons (the mean number of LFP channels recorded per mouse). A corrected *p* value < 0.05 was considered significant. All comparisons across genotype were made against WT littermate controls.

Results

WT mice display neural phase signaling

First, we investigated whether WT mice displayed neural phase synchrony across the HP–PF pathway during behavioral explo-

ration. We simultaneously recorded local field potentials (LFPs) from HP and PrL as mice explored a novel environment. To measure low- and high-frequency phase synchrony across the HP–PF pathway, we bandpass filtered LFPs in the theta (4–10 Hz) or gamma (33–55 Hz) range, and decomposed filtered oscillations into instantaneous phase and amplitude components (Fig. 1*a*). We then quantified theta and gamma band phase synchrony by calculating the circular uniformity of the phase time series difference between the HP and PrL electrode pairs (Fig. 1*b*,*c*). Using this process, we identified significant theta band and gamma band phase synchrony across the HP–PF pathway (Fig. 1*d*–*g*). Incidentally, we also investigated theta and gamma band phase synchrony during periods of quiet waking (behaviorally inactive) while WT mice were in their home cage. Our results indicated that novelty exposure significantly increased theta band synchrony (theta *Z*-stat: 12,910 ± 490 in the novel environment, 2960 ± 170 in the home cage; $t\text{-stat}_{(1,510)} = 15.2$; $p < 0.001$), and decreased gamma band synchrony in WT mice (gamma *Z*-stat: 1350 ± 100 in the novel environment, 3180 ± 210 in the home cage; $t\text{-stat}_{(1,510)} = 9.02$; $p < 0.001$).

Next, we quantified HP and PrL intrastructural synchrony by calculating theta-gamma CFPC using the modulation index (Fig. 2*a*–*b*) (Canolty et al., 2006). Our results indicated that WT mice displayed significant HP and PrL intrastructural synchrony during periods of novel exploration. Moreover, our results also indicated that novelty exposure significantly increased hippocampal and cortical CFPC in WT mice when compared with periods of behavioral inactivity while mice were in their home cage ($t\text{-stat}_{(1,58)} = 2.46$; $p < 0.05$ and $t\text{-stat}_{(1,61)} = 4.87$; $p < 0.001$, respectively) (Fig. 2*c*–*d*). Finally, to quantify the influence of hippocampal theta oscillatory activity over cortical gamma oscillatory activity, we calculated interstructural CFPC using the modulation Index. Consistent with previous reports (Sirota et al., 2008), our results indicated that WT mice displayed significant phase coupling between cortical gamma oscillations and hippocampal theta oscillations during periods of novel exploration. Our results also indicated that novelty exposure significantly increased interstructural CFPC when compared with periods of behavioral inactivity while mice were in their home cage (*M*: 0.9 ± 0.0 in the home cage, 1.7 ± 0.1 in the novel environment; $t\text{-stat}_{(1,470)} = 8.81$, $p < 0.000001$) (Fig. 2*e*).

After demonstrating that neural phase

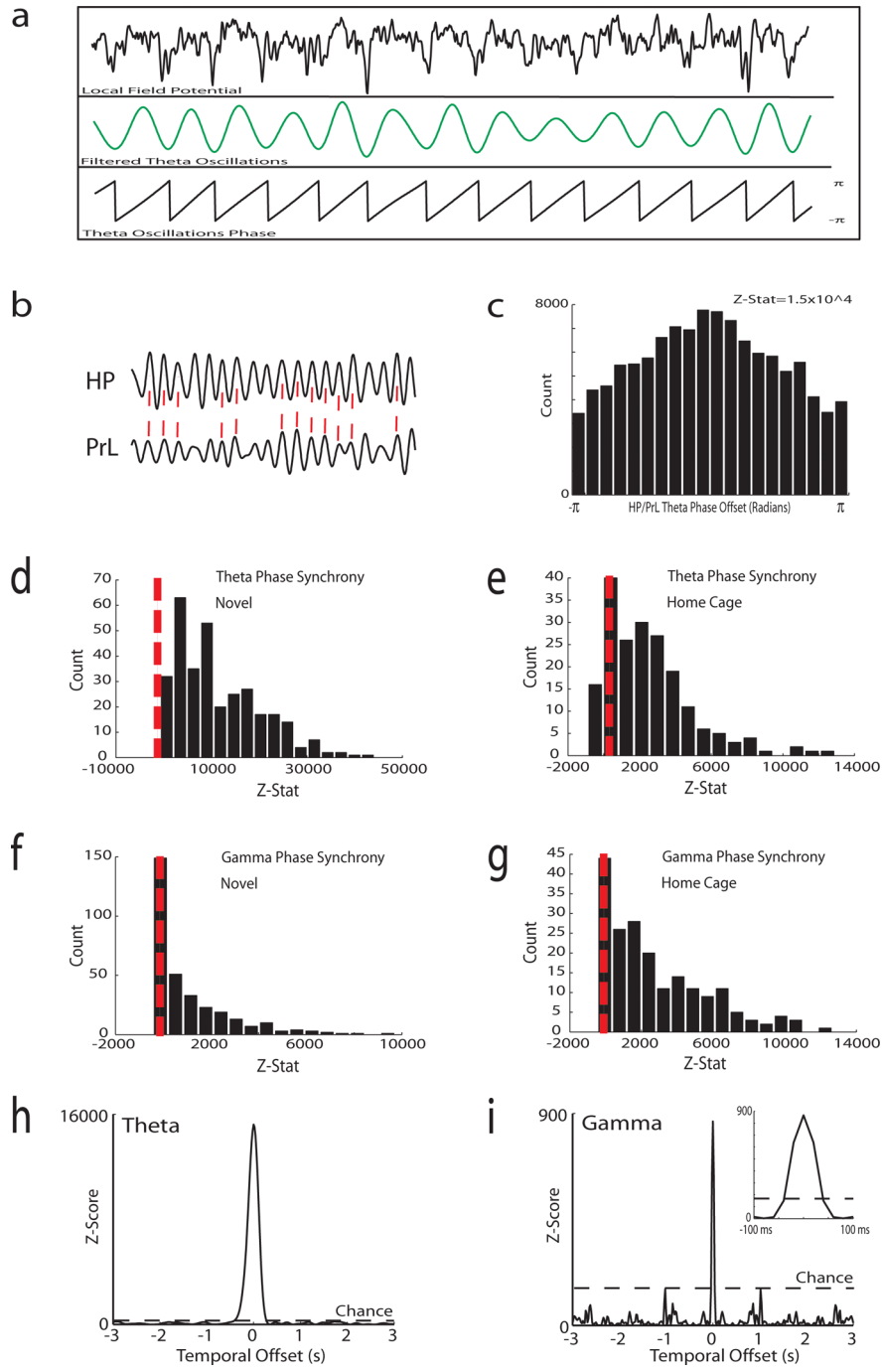

Figure 1. Low- and high-frequency phase synchrony across the hippocampus–prefrontal cortex pathway. Electrophysiological recordings were conducted in WT mice as they explored a novel environment. ***a***, Hippocampus and prelimbic cortex LFP oscillations were filtered in the theta (4–10 Hz) and gamma (33–55 Hz) frequency range, and phase time series were extracted via Hilbert transform. ***b***, Three second trace of theta filtered HP and PrL LFP oscillations demonstrating periods of instantaneous phase synchrony (denoted by red dashes). ***c***, Histogram of all of the instantaneous theta phase offset values observed between a single HP and PrL electrode pair. Phase synchrony was quantified for each HP and PrL electrode pair by calculating the Rayleigh statistic for the instantaneous phase offset values observed between the two electrodes within the frequency range of interest, where the *Z*-stat = $-\ln(P)$. ***d–g***, Distribution of *Z*-stats corresponding to (***d***, ***e***) theta band and (***f***, ***g***) gamma band phase synchrony values measured across all HP-PrL electrode pairs while WT mice were in the novel environment (left) and home cage (right). All of the HP-PrL combinations (320/320) demonstrated significant theta band phase synchrony in the novel environment. Novelty exposure significantly enhanced theta band phase synchrony when compared with theta band phase synchrony values measured while mice were in their home cage. The majority of HP-PrL LFP combinations (285/320) demonstrated significant gamma band phase synchrony. Novelty exposure significantly diminished gamma band phase synchrony when compared with gamma band phase synchrony values measured while mice were in their home cage. ***h***, Introduction of temporal offsets >500 ms between HP and PrL LFP's abolished theta phase synchrony. ***i***, Introduction of temporal offsets >40 ms between HP and PrL LFP's abolished gamma phase synchrony (see inset).

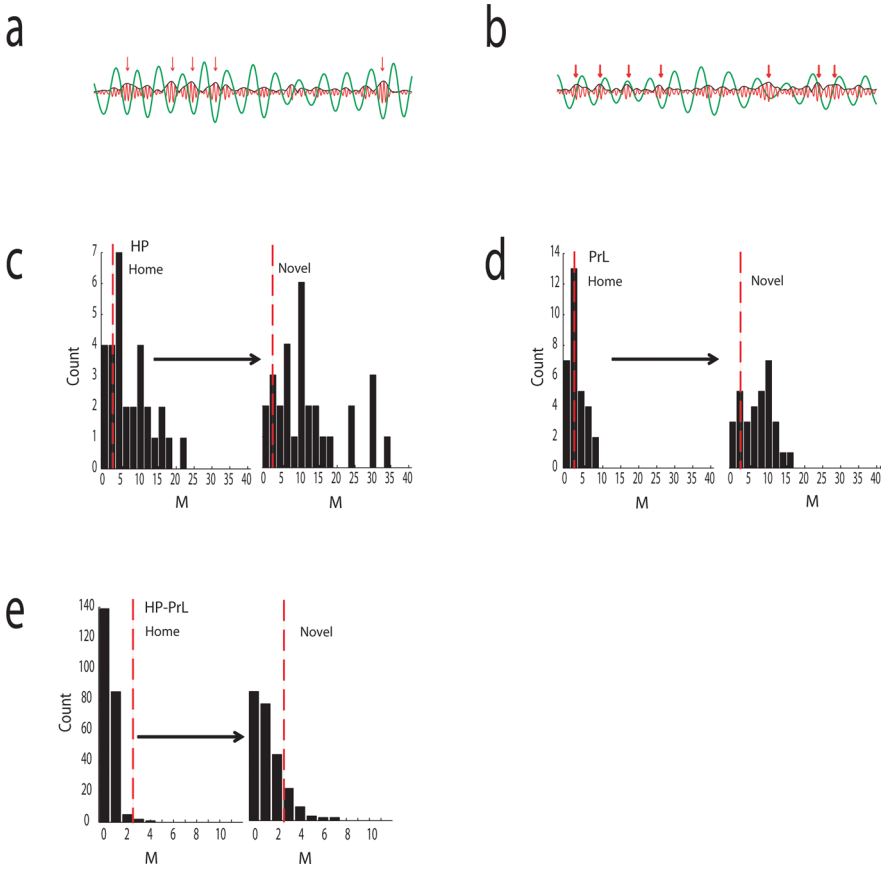

Figure 2. Phasic modulation of gamma oscillations by theta oscillations. ***a***, Two second hippocampal theta oscillation trace (green) overlaid on simultaneously recorded gamma oscillations (red) and the gamma oscillation amplitude envelope (black). Red arrows show bouts of increased gamma oscillation amplitudes that were phase coupled to theta oscillation troughs. ***b***, Sample of hippocampal LFP channel that did not display theta-gamma coupling. Notice peaks in gamma oscillatory power are not consistent with a theta oscillation phase. ***c***, ***d***, The modulation index *M* was determined for all hippocampal (***c***) and cortical LFP channels (***d***) while mice were in their home cage and exploring a novel environment. Novelty exposure potentiated hippocampal and cortical theta-gamma coupling in WT mice. ***e***, Coupling between hippocampal theta oscillations and cortical gamma oscillations was quantified using the modulation index *M*. Only 2/232 HP-PrL channel combinations demonstrated significant modulation in the home cage; conversely, 39/240 HP-PrL channel combinations demonstrated significant theta-gamma modulation in the novel environment.

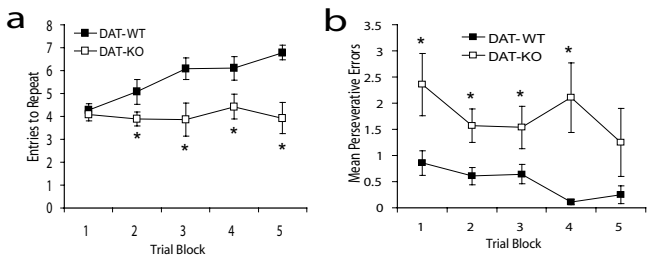

Figure 3. Persistent hyperdopaminergia disrupts spatial cognitive performance. Spatial cognitive performance was measured using an eight-arm radial maze task across five 4 d trial blocks. ***a***, ***b***, DAT-KO mice displayed deficits in cognitive performance as measured by the number of arms entered before a repeat entry (***a***) and cognitive inflexibility as measured by the number of perseverative errors committed during task performance (***b***). Data are presented as mean ± SEM; $n = 7$ for both groups. *$p < 0.05$ for single comparisons across genotype using ANOVA followed by Student's *t* test.

signaling was indeed present in WT mice, we investigated whether specific aspects of neural phase signaling were altered by persistent hyperdopaminergia or NMDA receptor hypofunction.

Hyperdopaminergia increases gamma phase signaling

To assess spatial cognitive function in dopamine transporter-knock-out (DAT-KO) mice, we subjected mice to a classic eight-arm radial maze learning task. Our results indicated that C57BL/6J DAT-KO mice displayed deficits in spatial cognitive performance. As shown in Figure 3, two-way ANOVA of the entries to repeat found the main effects of genotype ($F_{(1,69)} = 11.09$, $p < 0.01$) and trial ($F_{(4,69)} = 3.53$, $p = 0.013$), as well as the genotype by condition interaction ($F_{(4,69)} = 3.46$, $p = 0.014$) to be significant. Moreover, two-way ANOVA of the perseverative errors committed found the main effects of genotype ($F_{(1,69)} = 11.60$, $p < 0.01$) to be significant. These observations, which are consistent with observations previously gained in DAT-KO mice bred on a different background (129×C57BL6 mixed background) (Gainetdinov et al., 1999), indicate that altered dopamine signaling leads to cognitive dysfunction.

After confirming that DAT-KO mice displayed spatial cognitive deficits compared with their WT littermates, we set out to quantify HP–PF phase signaling during spatial cognitive processing in the mutant mice. DAT-KO mice were surgically implanted with microwire electrodes, and LFP recordings were conducted as they engaged in novelty induced exploration. We found that DAT-KO mice displayed significantly higher HP-PrL gamma band phase synchrony compared with WT mice during exploration of a novel environment (DAT-KO gamma *Z*-stat: 3640 ± 310; $n = 296$ channel combinations, $t\text{-stat}_{(1,614)} = 7.26$, $p < 0.0000001$, compared with novelty exposed WT mice) (compare Figs. 1 and 4*c*). Conversely, theta band phase synchrony was statistically indistinguishable in DAT-KO and WT mice (DAT-KO theta *Z*-stat: 12,740 ± 700; $n = 296$ channel combinations, $t\text{-stat}_{(1,614)} = 0.20$, $p > 0.05$ compared with novelty exposed WT mice) (compare Figs. 1 and 4*a*). When we compared these data to LFP recordings conducted while DAT-KO mice were in their home cage, we found that novelty exposure potentiated theta band phase synchrony ($t\text{-stat}_{(1,534)} = 10.88$, $p < 0.001$), but failed to attenuate HP–PF gamma band phase synchrony as it had in WT mice ($t\text{-stat}_{(1,534)} = 0.98$; $p > 0.05$). Interestingly, our results also showed that hippocampal and cortical theta-gamma CFPC in DAT-KO mice and interstructural CFPC (hippocampal theta − cortical gamma coupling) was statistically indistinguishable from that observed in WT mice ($p > 0.05$ for all comparisons).

To investigate the increased HP–PF gamma phase synchrony in DAT-KO mice, we measured HP-PrL PDC. PDC is a method that quantifies the preferential direction of wave activity propagation between two fields based on power spectral changes (Sameshima and Baccalá, 1999; Baccalá and Sameshima, 2001; Kuś et al., 2004; Baccalá et al., 2006; Takahashi et al., 2007). DAT-KO mice displayed increased PrL to HP directional wave

propagation in the high frequency range compared with WT mice (t-stat$_{(1,29)}$ = 5.78, respectively, $p < 0.01$).

Conversely, there was no difference in high frequency HP to PrL wave propagation (Fig. 4*e*). Together, this suggests that HP gamma oscillatory activity becomes increasingly synchronized to the gamma source responsible for modulating high frequency PrL oscillatory activity in DAT-KO mice.

Overall, our data demonstrated that persistent hyperdopaminergia alters high frequency interstructural HP–PF synchrony, while leaving low frequency interstructural HP–PF synchrony and HP–PF intrastructural synchrony intact.

NMDA receptor hypofunction disrupts theta-gamma phase coupling

Since the spatial cognitive processing of NR1-KD mutants had not been assessed, we subjected WT and NR1-KD mice to our radial-arm maze spatial learning task (Fig. 5). Two-way ANOVA of entries to repeat found the main effects of genotype ($F_{(1,74)} = 14.01$, $p < 0.001$) but not trial ($F_{(4,74)} = 1.36$, $p > 0.05$), or the genotype by condition interaction ($F_{(4,74)} = 0.93$, $p > 0.05$) to be significant. This was caused by the rapid learning rates observed in 5/7 WT mice observed across the first block. When entries to repeat analysis was limited to data collected on the first day of each trial block, two-way ANOVA found the main effects of genotype ($F_{(1,74)} = 16.95$, $p < 0.01$) and trial ($F_{(4,74)} = 4.30$, $p < 0.01$), as well as the genotype by condition interaction ($F_{(4,74)} = 3.36$, $p = 0.016$) to be significant. Moreover, two-way ANOVA of perseverative errors found the main effects of genotype ($F_{(1,69)} = 37.91$, $p < 0.001$) to be significant, demonstrating that NR1-KD mice displayed cognitive inflexibility (Clarke et al., 2004). Together, these results indicated that global NMDA receptor hypofunction was indeed associated with cognitive dysfunction.

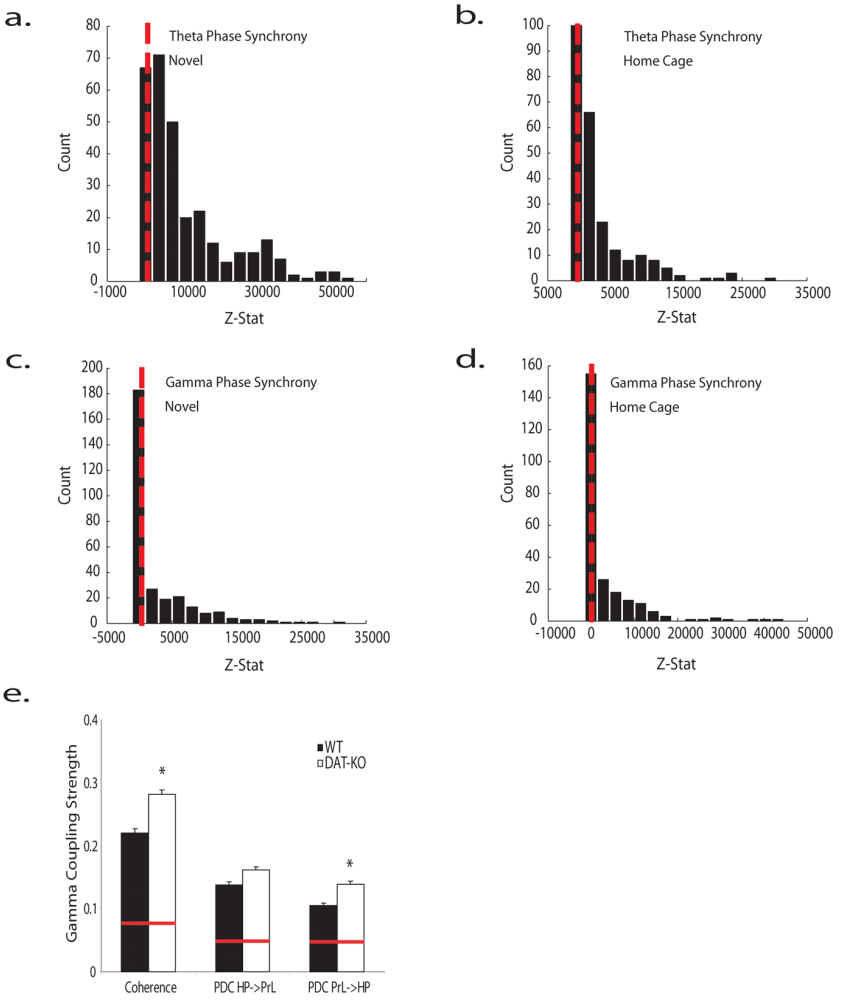

Figure 4. HP-PrL gamma phase synchrony is potentiated in DAT-KO mice. Electrophysiological recordings were conducted in WT mice as they explored a novel environment. ***a–d***, Distribution of *Z*-stat corresponding to theta band (***a***, ***b***) and gamma band (***c***, ***d***) phase synchrony values measured across all HP-PrL electrode pairs while mice were in the novel environment (left) and home cage (right). DAT-KO mice displayed significantly higher HP-PrL gamma phase synchrony than novelty exposed WT mice. Theta band phase synchrony remained unchanged. ***e***, Novelty exposure increased theta-band synchrony in DAT-KO mice but failed to attenuate gamma band phase synchrony. Gamma band HP-PrL coherence and PrL to HP partial directed LFP coherence was significantly increased in DAT-KO mice. Red bars indicate significance thresholds at $^*p < 0.01$.

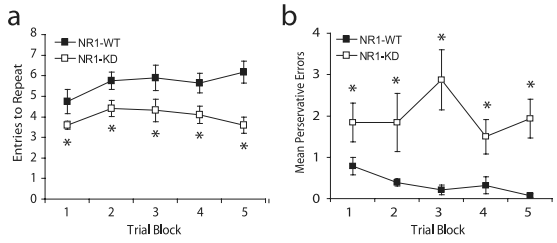

Figure 5. NMDA receptor hypofunction disrupts hippocampal and prefrontal cortical-dependent cognitive function. Spatial cognitive performance was measured using an eight-arm radial maze task across five 4 d trial blocks. ***a***, ***b***, NR1-KD mice displayed deficits in cognitive performance as measured by the number of arms entered before a repeat entry (***a***) and cognitive inflexibility as measured by the number of perseverative errors committed during task performance (***b***). Data are presented as mean ± SEM; $n = 7$ and 8 for WT and NR1-KD mice, respectively. $^*p < 0.05$ for single comparisons across genotype using mixed ANOVA followed by Student's t test.

After confirming that NR1-KD mice displayed spatial cognitive deficits compared with their WT littermates, we set out to quantify whether HP–PF phase signaling was altered during periods of spatial cognitive processing in the mutant mice. NR1-KD mice were surgically implanted with microwire electrodes, and LFP recordings were conducted as they engaged in novelty induced exploration. NR1-KD mice displayed HP–PF theta and gamma band phase synchrony that was statistically indistinguishable from that observed in WT mice ($p > 0.05$ for both comparisons). Conversely, NR1-KD mice displayed profound deficits in hippocampal and prelimbic cortical theta-gamma CFPC compared with WT mice during periods of novel exploration (t-stat$_{(1,66)} = 13.83$ and t-stat$_{(1,70)} = 8.18$, respectively, $p < 0.001$ for both comparisons) (compare Figs. 2 and 6*a*,*b*). Our data recorded from NR1-KD mice during periods of quiet waking in their home cage also demonstrated that novelty exposure failed to potentiate HP and PrL CFPC as it had in WT mice (t-stat$_{(1,60)} = 0.63$ and t-stat$_{(1,60)} = 0.77$, respectively; $p > 0.05$) (Fig. 6*a*,*b*). Importantly, these deficits were not attributable to changes in hippocampal/prelimbic cortical theta or gamma oscillatory power (see supplemental Figs. S8, S9, available at www.jneurosci.org as

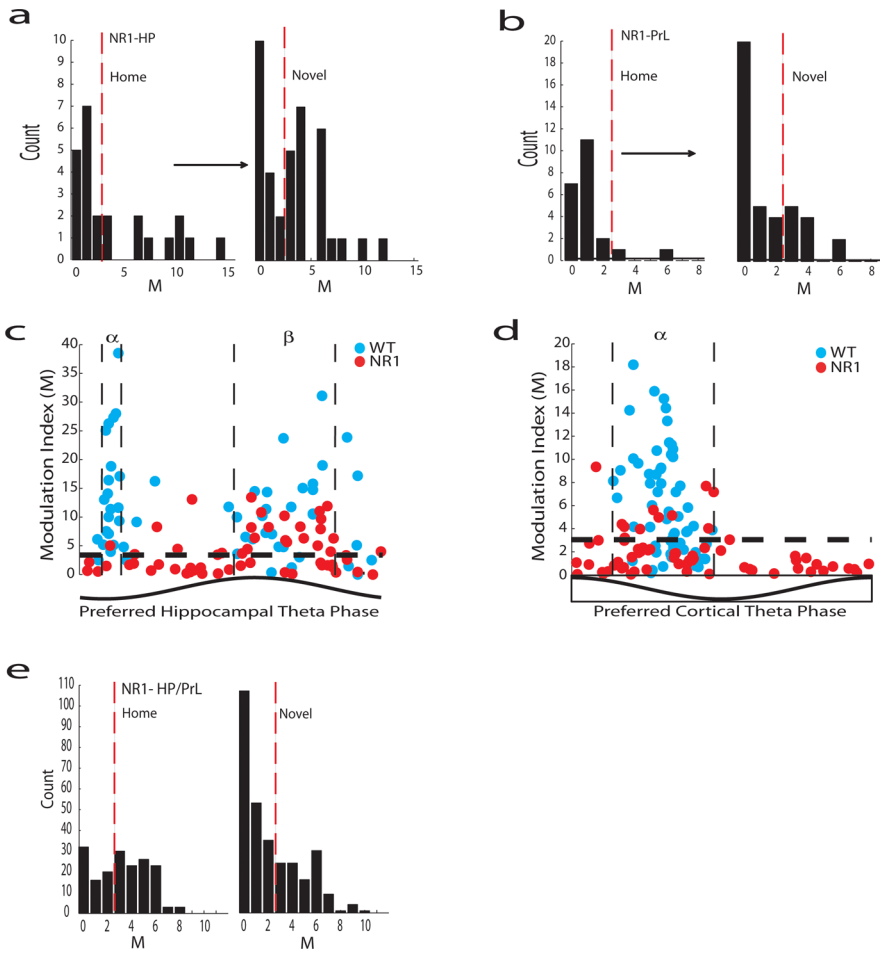

Figure 6. NR1-KD mice displayed attenuated theta-gamma phase coupling. Electrophysiological recordings were conducted in WT mice as they explored a novel environment. ***a***, ***b***, NR1-KD displayed significantly attenuated hippocampal (***a***) and cortical (***b***) theta-gamma coupling compared with WT mice. Additionally, novelty exposure failed to potentiate hippocampal and cortical theta-gamma coupling strength in NR1-KD mice when compared with data recorded while mice were in their home cage. ***c***, Phase modulation of hippocampal LFP channels clustered at two preferred phases in WT mice (α and β, demarcated by vertical dashed lines). NR1-KD mice displayed disrupted hippocampal α phase but not β phase modulation. Each WT animal had multiple hippocampal LFP channels that displayed α phase modulation. ***d***, Phase modulation of cortical LFP channels occurred at one preferred phase in WT and NR1-KD mice (α, demarcated by vertical dashed lines). ***e***, Coupling between hippocampal theta oscillations and cortical gamma oscillations was quantified using the modulation index *M*. NR1-KD mice displayed enhanced interstructural theta-gamma modulation in the novel environment (111/304 significantly modulated channel combinations) and home cage (111/176 significantly modulated channel combinations) compared with WT mice.

supplemental material). When data recorded from WT mice was pooled across all sessions, we found that hippocampal gamma oscillatory power was preferentially modulated by a precise phase band of the theta oscillation trough and a broad phase band after the theta oscillation peak. All of the WT mice displayed preferential gamma modulation at both the precise and broad phase band; conversely, NR1-KD mice only showed preferential modulation of gamma oscillatory activity by a broad phase band after the theta oscillation peak (Fig. 6*c*). These results suggest that NMDA receptor function is critically involved in coordinating processes central to the precise coupling of gamma oscillatory power to the theta oscillation trough. Our results also showed that cortical gamma oscillatory power in WT mice was preferentially modulated by a broad phase band during the falling phase of theta oscillations. Similarly, NR1-KD mice showed preferential modulation of gamma oscillatory power by a broad phase band during the falling phase of theta oscillations, although cortical CFPC was significantly diminished overall (Fig. 6*d*). Next, we investigated interstructural phase coupling (hippocampal theta-cortical gamma) in NR1-KD mice. Our results indicated that novelty exposed NR1-KD mice displayed significantly enhanced interstructural CFPC compared with their WT littermate controls. Moreover, enhanced interstructural CFPC was also observed during quiet waking while NR1-KD mice were in their home cage (NR1-Novel *M*: 2.7 ± 0.1, NR1-Home *M*: 3.6 ± 0.2, $t\text{-stat}_{(1,478)} = 4.23$, $p < 0.0001$ for both comparisons) (compare Figs. 2*e* and 6*e*).

Together, our data suggested that NMDA receptor hypofunction disrupts HP and PF intrastructural coupling between theta and gamma oscillations while enhancing interstructural coupling between hippocampal theta and cortical gamma oscillatory activity (Fig. 7).

Discussion

Spatial cognitive processing and hippocampus–prefrontal cortex phase signaling

Neural phase signaling has gained attention as a putative coding mechanism through which the brain binds the activity of neurons across distributed brain structures to generate thoughts, percepts, and behaviors. Several studies in rodents have been aimed at investigating HP–prefrontal cortex pathway phase signaling during spatial cognitive processes. These studies have shown that both HP and PF neurons (Siapas et al., 2005), and HP–PF gamma oscillatory activity (Sirota et al., 2008), phase lock to HP theta oscillations during periods of exploration in a novel environment. Moreover, studies have demonstrated that HP and PF theta oscillations phase synchronize during accurate spatial task performance (Jones and Wilson, 2005), suggesting that phase signaling plays an important role in coordinating HP–PF pathway function during periods of enhanced spatial cognitive processing.

Here, we identify altered phase signaling across the hippocampus–prefrontal cortex pathway in two mouse models of cognitive dysfunction: mice with genetically induced hyperdopaminergia (DAT-KO mice) and mice with genetically induced NMDA receptor hypofunction (NR1-KD mice). Although our findings only serve to correlate deficits in HP–PF phase signaling with gross dysfunction in spatial cognitive task performance, they provide a novel frame work to investigate the molecular mechanisms underlying phase signaling, and ultimately the role that phase signaling plays in coordinating brain activity during spatial cognitive processing.

Gamma phase coupling is not caused by signal artifact

Our findings indicated that WT mice display theta and gamma band phase synchrony at zero lag. Zero lag phase synchrony can result from defined neurological mechanisms, or from artifacts such as generic noise or electrical diffusion. Although our data demonstrating the presence of HP and PrL theta-gamma cou-

pling in WT mice suggested that theta band phase synchrony was not simply caused by mechanical noise, our findings did not exclude the possibility that the theta band zero-lag phase synchrony measured using our recording technique may have resulted from electrical diffusion (Sirota et al., 2008). Thus, DAT-KO and NR1-KD mice may have indeed displayed alterations in theta-band synchrony that were not identified in this study. However, our findings did suggest that gamma band phase synchrony resulted from neurological mechanisms. First, gamma oscillations are local (Sirota et al., 2008), Thus, it is unlikely that hippocampal gamma oscillations could be recorded from PrL cortex given the distance between the two structures. Second, our analysis demonstrated that there was limited coherence at frequencies between theta and gamma coherence bands (see supplemental Fig. S4, available at www.jneurosci.org as supplemental material). Given that WT and DAT-KO (Dzirasa et al., 2006), and NR1-KD mice (see supplemental Fig. S5, available at www.jneurosci.org as supplemental material) both display higher hippocampal power at frequencies ranging from 10 to 33 Hz than the gamma frequency range, a continuous coherence band from 4 to 55 Hz would be observed if the gamma coherence observed throughout the study was attributable to electrical diffusion. Finally, we found a high coefficient of variance of gamma phase synchrony across HPxPrL channel combinations even within the same mice. In fact, we even found channel combinations that displayed high phase synchrony and channel combinations that displayed no phase synchrony at all in the same mice. If gamma phase synchrony was attributable to electrical diffusion, common noise, or technical cross talk, gamma phase synchrony would be detected in all of the channel combinations.

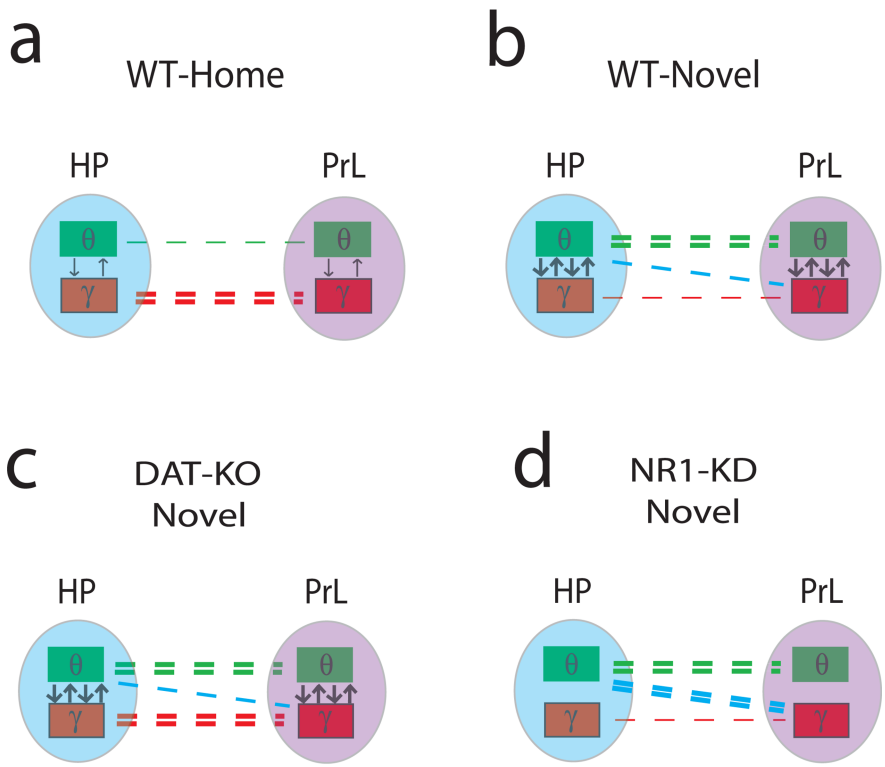

Figure 7. Model of novelty, dopamine, and NMDA receptor hypofunction effects on neural phase signaling. ***a***, WT mice show high HP–PF gamma band synchrony, low HP–PF theta band phase synchrony, and low theta-gamma phase coupling in their home cage. ***b***, Novelty exposure potentiates HP–PF theta band synchrony, theta-gamma intrastructural phase coupling, theta-gamma interstructural phase coupling, and attenuates HP–PF gamma band synchrony in WT mice. ***c***, HP–PF gamma band interstructural phase synchrony is potentiated in DAT-KO mice. ***d***, HP and PF intrastructural phase coupling is disrupted in NR1-KD mice, and HP and PF interstructural phase coupling is enhanced in NR1-KD mice.

Persistent hyperdopaminergia and NMDA receptor hypofunction selectively disrupt gamma phase signaling

Our data demonstrated that novelty exposure increased HP–PF theta phase synchrony and theta-gamma intrastructural phase coupling in normal mice. Thus, theta phase synchrony and intrastructural phase coupling likely plays a prominent role in coordinating hippocampal and cortical gamma oscillatory activity during periods of behavioral exploration. Conversely, novelty exposure decreased gamma band internetwork phase synchrony. Our results in DAT-KO mice demonstrate that persistent hyperdopaminergia potentiates HP–PF gamma band interstructural phase synchrony. We also show that the enhanced HP–PF gamma band phase synchrony observed in DAT-KO mice is associated with a unidirectional increase in gamma band LFP wave propagation from PrL to HP. Thus, our findings suggest that persistent hyperdopaminergia enhances the synchronization of hippocampal oscillations to the gamma source responsible for generating PF gamma oscillatory activity. Incidentally, hippocampal gamma oscillatory activity becomes phase synchronized to cortical gamma oscillations as learning progresses (Fell et al., 2001), and evidence suggests that this process may be mediated by efferent projections from prefrontal cortex to lateral entorhinal cortex that control the transfer of information from hippocampus to cortex (Paz et al., 2007). Moreover, several studies indicate that modest increases in dopaminergic tone enhance neuronal activity in entorhinal cortex (Caruana et al., 2006), and DAT-KO mice have been shown to display increased gamma oscillatory power across hippocampus (Dzirasa et al., 2006). Thus, the increased HP–PF gamma band synchrony observed in DAT-KO mice may be attributable to enhanced dopaminergic activity at entorhinal cortex. Importantly, our results also demonstrate that hyperdopaminergia does not alter HP-PrL theta band phase synchrony or HP and PrL intrastructural synchrony. Together, these results suggest that HP-PrL gamma-band phase synchrony represents an independent mechanism for processing high frequency information across the HP–PF pathway.

Our results observed in the NR1-KD mice also showed that diminished NMDA receptor function disrupts hippocampal and cortical intrastructural synchrony, while enhancing interstructural CFPC and leaving low- and high-frequency interstructural phase synchrony intact. This indicates that the interstructural synchronization of HP–PF gamma oscillatory activity does not simply result from coordinated theta-gamma interactions occurring locally within each of these two structures. Rather, our data collected in NR1-KD mice also suggests that gamma-band phase synchrony results from a complex mechanism responsible for coordinating high precision information processing across the HP–PF pathway.

Altogether, our findings suggest that gamma-band phase syn-

chrony and theta-gamma phase coupling likely represent distinct phase signaling mechanisms for binding the activity of interstructural and intrastructural neuronal populations. Moreover, the coordination of gamma oscillatory activity using these phase signaling mechanisms is differentially affected by novelty, persistent hyperdopaminergia, and NMDA receptor hypofunction.

Hyperdopaminergia, NMDA receptor hypofunction, and human cognitive dysfunction

DA signaling has been suspected as an important mediator of the cognitive function (Kellendonk et al., 2006), and glutamatergic signaling has been shown to play an important role in learning and memory via activation of NMDA receptors (Larson and Lynch, 1988; O'Dell et al., 1991; Tsien et al., 1996; Tang et al., 1999; Shimizu et al., 2000). As such, it is believed that alterations in dopamine and/or NMDA receptor dependant glutamate neurotransmission contribute, at least in part, to the cognitive endophenotypes observed across neuropsychiatric disorders such as schizophrenia, attention-deficit-hyperactivity disorder, and bipolar disorder (Coyle, 1996; Tamminga, 1998; Laruelle and Abi-Dargham, 1999; Coyle and Tsai, 2004; Horschitz et al., 2005; Jucaite et al., 2005; Kellendonk et al., 2006). Although the electrophysiological mechanisms underlying the manifestation of these brain disorders have yet to be identified, multiple studies have demonstrated that the cognitive impairments observed in patients with schizophrenia are associated with altered coordination of high frequency neural oscillatory activity (Spencer et al., 2004; Cho et al., 2006; Light et al., 2006; Yeragani et al., 2006). Moreover, several electroencephalographic studies have demonstrated that individuals with schizophrenia display abnormal activation of prefrontal cortical networks during cognitive tasks (Winterer et al., 2000, 2004). Together with our findings, this suggests that altered high frequency phase signaling may indeed play a role in mediating cognitive dysfunction; however, further studies will be necessary to definitively test this critical assumption.

References

Baccalá LA, Sameshima K (2001) Partial directed coherence: a new concept in neural structure determination. Biol Cybern 84:463–474.

Baccalá LA, Takahashi YD, Sameshima K (2006) Computer intensive testing for the influence between time series. In: Handbook of time series analysis (Schelter B, Winterhalder M, Timmer J, eds), pp 411–433. Weinheim, Germany: Wiley–VCH Verlag.

Bendat JS, Piersol AG (1986) Random data: analysis and measurement procedures, Ed 2. New York: Wiley.

Bragin A, Jandó G, Nádasdy Z, Hetke J, Wise K, Buzsáki G (1995) Gamma (40–100 Hz) oscillation in the hippocampus of the behaving rat. J Neurosci 15:47–60.

Canolty RT, Edwards E, Dalal SS, Soltani M, Nagarajan SS, Kirsch HE, Berger MS, Barbaro NM, Knight RT (2006) High gamma power is phase-locked to theta oscillations in human neocortex. Science 313:1626–1628.

Caruana DA, Sorge RE, Stewart J, Chapman CA (2006) Dopamine has bidirectional effects on synaptic responses to cortical inputs in layer II of the lateral entorhinal cortex. J Neurophysiol 96:3006–3015.

Cho RY, Konecky RO, Carter CS (2006) Impairments in frontal cortical gamma synchrony and cognitive control in schizophrenia. Proc Natl Acad Sci U S A 103:19878–19883.

Chrobak JJ, Buzsáki G (1998) Gamma oscillations in the entorhinal cortex of the freely behaving rat. J Neurosci 18:388–398.

Clarke HF, Dalley JW, Crofts HS, Robbins TW, Roberts AC (2004) Cognitive inflexibility after prefrontal serotonin depletion. Science 304:878–880.

Coyle JT (1996) The glutamatergic dysfunction hypothesis for schizophrenia. Harv Rev Psychiatry 3:241–253.

Coyle JT, Tsai G (2004) The NMDA receptor glycine modulatory site: a therapeutic target for improving cognition and reducing negative symptoms in schizophrenia. Psychopharmacology 174:32–38.

Duncan GE, Moy SS, Lieberman JA, Koller BH (2006) Effects of haloperidol, clozapine, and quetiapine on sensorimotor gating in a genetic model of reduced NMDA receptor function. Psychopharmacology 184:190–200.

Dzirasa K, Ribeiro S, Costa R, Santos LM, Lin SC, Grosmark A, Sotnikova TD, Gainetdinov RR, Caron MG, Nicolelis MA (2006) Dopaminergic control of sleep–wake states. J Neurosci 26:10577–10589.

Fell J, Klaver P, Lehnertz K, Grunwald T, Schaller C, Elger CE, Fernández G (2001) Human memory formation is accompanied by rhinal-hippocampal coupling and decoupling. Nat Neurosci 4:1259–1264.

Forrest D, Yuzaki M, Soares HD, Ng L, Luk DC, Sheng M, Stewart CL, Morgan JI, Connor JA, Curran T (1994) Targeted disruption of NMDA receptor 1 gene abolishes NMDA response and results in neonatal death. Neuron 13:325–338.

Gainetdinov RR, Caron MG (2003) Monoamine transporters: from genes to behavior. Annu Rev Pharmacol Toxicol 43:261–284.

Gainetdinov RR, Wetsel WC, Jones SR, Levin ED, Jaber M, Caron MG (1999) Role of serotonin in the paradoxical calming effect of psychostimulants on hyperactivity. Science 283:397–401.

Giros B, Jaber M, Jones SR, Wightman RM, Caron MG (1996) Hyperlocomotion and indifference to cocaine and amphetamine in mice lacking the dopamine transporter. Nature 379:606–612.

Horschitz S, Hummerich R, Lau T, Rietschel M, Schloss P (2005) A dopamine transporter mutation associated with bipolar affective disorder causes inhibition of transporter cell surface expression. Mol Psychiatry 10:1104–1109.

Jacobs J, Kahana MJ, Ekstrom AD, Fried I (2007) Brain oscillations control timing of single-neuron activity in humans. J Neurosci 27:3839–3844.

Jones MW, Wilson MA (2005) Theta rhythms coordinate hippocampal-prefrontal interactions in a spatial memory task. PLoS Biol 3:e402.

Jucaite A, Fernell E, Halldin C, Forssberg H, Farde L (2005) Reduced midbrain dopamine transporter binding in male adolescents with attention-deficit/hyperactivity disorder: association between striatal dopamine markers and motor hyperactivity. Biol Psychiatry 57:229–238.

Kellendonk C, Simpson EH, Polan HJ, Malleret G, Vronskaya S, Winiger V, Moore H, Kandel ER (2006) Transient and selective overexpression of dopamine D2 receptors in the striatum causes persistent abnormalities in prefrontal cortex functioning. Neuron 49:603–615.

Kuś R, Kamiński M, Blinowska KJ (2004) Determination of EEG activity propagation: pair-wise versus multichannel estimate. IEEE Trans Biomed Eng 51:1501–1510.

Kutsuwada T, Kashiwabuchi N, Mori H, Sakimura K, Kushiya E, Araki K, Meguro H, Masaki H, Kumanishi T, Arakawa M, Mishina M (1992) Molecular diversity of the NMDA receptor channel. Nature 358:36–41.

Larson J, Lynch G (1988) Role of N-methyl-D-aspartate receptors in the induction of synaptic potentiation by burst stimulation patterned after the hippocampal theta-rhythm. Brain Res 441:111–118.

Laruelle M, Abi-Dargham A (1999) Dopamine as the wind of the psychotic fire: new evidence from brain imaging studies. J Psychopharmacol 13:358–371.

Li Y, Erzurumlu RS, Chen C, Jhaveri S, Tonegawa S (1994) Whisker-related neuronal patterns fail to develop in the trigeminal brainstem nuclei of NMDAR1 knockout mice. Cell 76:427–437.

Light GA, Hsu JL, Hsieh MH, Meyer-Gomes K, Sprock J, Swerdlow NR, Braff DL (2006) Gamma band oscillations reveal neural network cortical coherence dysfunction in schizophrenia patients. Biol Psychiatry 60:1231–1240.

Lisman J, Buzsáki G (2008) A neural coding scheme formed by the combined function of gamma and theta oscillations. Schizophr Bull 34:974–980.

Mohn AR, Gainetdinov RR, Caron MG, Koller BH (1999) Mice with reduced NMDA receptor expression display behaviors related to schizophrenia. Cell 98:427–436.

Monyer H, Sprengel R, Schoepfer R, Herb A, Higuchi M, Lomeli H, Burnashev N, Sakmann B, Seeburg PH (1992) Heteromeric NMDA receptors: molecular and functional distinction of subtypes. Science 256:1217–1221.

Nelson MJ, Pouget P, Nilsen EA, Patten CD, Schall JD (2008) Review of signal distortion through metal microelectrode recording circuits and filters. J Neurosci Methods 169:141–157.

O'Dell TJ, Kandel ER, Grant SG (1991) Long-term potentiation in the hippocampus is blocked by tyrosine kinase inhibitors. Nature 353:558–560.

Palva JM, Palva S, Kaila K (2005) Phase synchrony among neuronal oscillations in the human cortex. J Neurosci 25:3962–3972.

Paz R, Bauer EP, Paré D (2007) Learning-related facilitation of rhinal interactions by medial prefrontal inputs. J Neurosci 27:6542–6551.

Rodriguez E, George N, Lachaux JP, Martinerie J, Renault B, Varela FJ (1999) Perception's shadow: long-distance synchronization of human brain activity. Nature 397:430–433.

Sameshima K, Baccalá LA (1999) Using partial directed coherence to describe neuronal ensemble interactions. J Neurosci Methods 94:93–103.

Seidenbecher T, Laxmi TR, Stork O, Pape HC (2003) Amygdalar and hippocampal theta rhythm synchronization during fear memory retrieval. Science 301:846–850.

Shimizu E, Tang YP, Rampon C, Tsien JZ (2000) NMDA receptor-dependent synaptic reinforcement as a crucial process for memory consolidation. Science 290:1170–1174.

Siapas AG, Lubenov EV, Wilson MA (2005) Prefrontal phase locking to hippocampal theta oscillations. Neuron 46:141–151.

Sirota A, Montgomery S, Fujisawa S, Isomura Y, Zugaro M, Buzsáki G (2008) Entrainment of neocortical neurons and gamma oscillations by the hippocampal theta rhythm. Neuron 60:683–697.

Spencer KM, Nestor PG, Perlmutter R, Niznikiewicz MA, Klump MC, Frumin M, Shenton ME, McCarley RW (2004) Neural synchrony indexes disordered perception and cognition in schizophrenia. Proc Natl Acad Sci U S A 101:17288–17293.

Takahashi DY, Bacca LA, Sameshima K (2007) Connectivity inference between neural structures via partial directed coherence. J Appl Stat 34:1259–1273.

Tamminga CA (1998) Schizophrenia and glutamatergic transmission. Crit Rev Neurobiol 12:21–36.

Tang YP, Shimizu E, Dube GR, Rampon C, Kerchner GA, Zhuo M, Liu G, Tsien JZ (1999) Genetic enhancement of learning and memory in mice. Nature 401:63–69.

Tsien JZ, Huerta PT, Tonegawa S (1996) The essential role of hippocampal CA1 NMDA receptor-dependent synaptic plasticity in spatial memory. Cell 87:1327–1338.

Winterer G, Ziller M, Dorn H, Frick K, Mulert C, Wuebben Y, Herrmann WM, Coppola R (2000) Schizophrenia: reduced signal-to-noise ratio and impaired phase-locking during information processing. Clin Neurophysiol 111:837–849.

Winterer G, Coppola R, Goldberg TE, Egan MF, Jones DW, Sanchez CE, Weinberger DR (2004) Prefrontal broadband noise, working memory, and genetic risk for schizophrenia. Am J Psychiatry 161:490–500.

Yeragani VK, Cashmere D, Miewald J, Tancer M, Keshavan MS (2006) Decreased coherence in higher frequency ranges (beta and gamma) between central and frontal EEG in patients with schizophrenia: a preliminary report. Psychiatry Res 141:53–60.